COMMUNICATION

ChemComm
www.rsc.org/chemcomm

Electronic and vibrational properties of a MOF-5 metal–organic framework: ZnO quantum dot behaviour

S. Bordiga,*[a] C. Lamberti,[a] G. Ricchiardi,[a] L. Regli,[a] F. Bonino,[a] A. Damin,[a] K.-P. Lillerud,[b] M. Bjorgen[b] and A. Zecchina*[a]

[a] *Dipartimento di Chimica IFM and NIS centre of excellence, Via P. Giuria 7, I-10125 Torino, Italy. E-mail: silvia.bordiga@unito.it; Fax: +39011-6707855; Tel: +39011-6707858*

[b] *Department of Chemistry, University of Oslo, P.O. Box 1033, N-0315 Oslo, Norway*

Received (in Cambridge, UK) 13th May 2004, Accepted 27th July 2004
First published as an Advance Article on the web 1st September 2004

UV–Vis DRS and photoluminescence (PL) spectroscopy, combined with excitation selective Raman spectroscopy, allow us to understand the main optical and vibrational properties of a metal–organic MOF-5 framework. A $O^{2-}Zn^{2+} \rightarrow O^{-}Zn^{+}$ ligand to metal charge transfer transition (LMCT) at 350 nm, testifies that the Zn_4O_{13} cluster behaves as a ZnO quantum dot (QD). The organic part acts as a photon antenna able to efficiently transfer the energy to the inorganic ZnO-like QD part, where an intense emission at 525 nm occurs.

Crystalline metal–organic frameworks (MOFs) represent a new class of porous materials constructed from transition metal ions and bridging organic ligands. MOFs have potential applications in separation, catalysis, nonlinear optics, and storage of gases.[1–9] The last generation open hybrid frameworks, emerging towards the end of the 1990s with the discovery of MOF-5 by Yaghi's group,[1] resulted in an important improvement of the framework stability. Stable MOF materials should open a new route to the design of crystals with flexible pore size, topology, and surface functionality.

Here we investigate vibrational and both absorption and emission electronic transitions on a MOF-5 material, synthesized according to ref. 10, using a Perkin-Elmer Lambda 15 DRS and a SPEX Fluorolog-2 PL spectrophotometer, respectively. Raman spectra were obtained using a Renishaw Micro-Raman System 1000 equipped with two different lasers able to generate three different lines: (i) an Argon laser, operating at 514 nm (19 455 cm^{-1}) and (ii) a He–Cd laser emitting at 325 nm (30 770 cm^{-1}) or at (iii) 442 nm (22 625 cm^{-1}). The photons scattered by the sample were dispersed by a grating monochromator and simultaneously collected on a CCD camera. The collection optic was a $\times 20$ objective. As model materials for the inorganic and organic parts of MOF-5, ZnO and a terephthalic acid disodium salt (TADS) have also been investigated.

Fig. 1(a) reports the UV–Vis DRS spectra of MOF-5 (solid curve), TADS (dotted curve) and ZnO (dashed curve). ZnO is classified as a wide band gap semiconductor as testified by the edge in the near UV region at 380 nm (26 300 cm^{-1}). As the valence and the conduction bands of ZnO are mainly due to O(2p) and Zn(4s) orbitals, respectively, this electronic transition can basically be described as an $O^{2-}Zn^{2+} \rightarrow O^{-}Zn^{+}$ LMCT. As can be seen in Fig. 1(a), TADS (dotted curve) exhibits an intense and complex absorption starting from 322 nm (31 000 cm^{-1}) and extending over the whole investigated UV region, ascribed to $\pi \rightarrow \pi^*$ electronic transitions of the aromatic ring. The red shift, with respect to the $\pi \rightarrow \pi^*$ transitions of benzene, is a consequence of the conjugation with the two $-CO_2^-$ carboxylate groups. In the case of MOF-5 (solid curve), we expect to observe contributions from both the organic linkers and the Zn_4O_{13} centers. The observed spectrum is actually complex, but not definitively given by the simple superimposition of the ZnO and the TADS signals. Two main features are observed: a maximum, centred at 290 nm (34 500 cm^{-1}), ascribable to the organic part, and an edge at 350 nm (28 600 cm^{-1}), due to the inorganic part. The edge at 350 nm (28 600 cm^{-1}), ascribed to a $O^{2-}Zn^{2+} \rightarrow O^{-}Zn^{+}$ LMCT, is blue shifted 2300 cm^{-1} with respect to the ZnO band gap due to confinement effects. As the external oxygens of the Zn_4O_{13} group belong to the carboxylate groups this cluster can be considered as a ZnO-like QD (Fig. 1(b)). This effect is similar to observations made for the ETS-10 titanosilicate, where the presence of a monoatomic –Ti–O–Ti–O– quantum wire causes a blue shift of the band gap of about 6800 cm^{-1} with respect to that of anatase.[11]

PL experiments were performed collecting both emission and excitation scans. The former are obtained by fixing the excitation

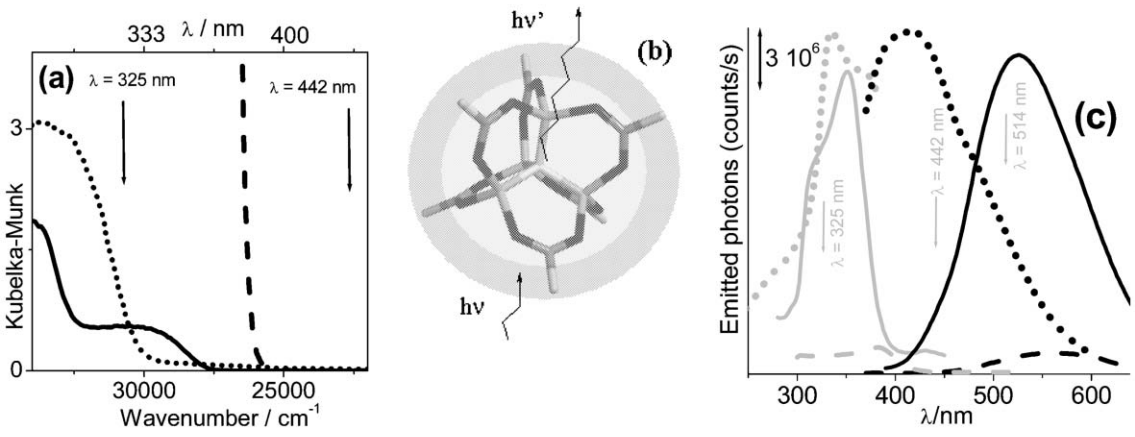

Fig. 1 Optical properties of MOF-5. (a) UV–Vis spectra of ZnO (dashed), TADS (dotted) and MOF-5 (solid). Arrows indicate Raman lasers. (b) Zn_4O_{13} group of MOF-5 Zn (light grey sticks) and O (dark grey sticks); benzene units (dangling white sticks), that act as photon absorbers ($h\nu$) are able to efficiently transfer the energy to the inorganic part where the photon emission occurs ($h\nu'$). (c) PL spectra. Grey curves (excitation scans), black curves (emission scans). MOF-5 (solid, $\lambda_{emis} = 518$ nm and $\lambda_{ex} = 350$ nm); TADS (dotted, $\lambda_{emis} = 418$ nm and $\lambda_{ex} = 335$ nm); ZnO (dashed, $\lambda_{emis} = 560$ nm and $\lambda_{ex} = 380$ nm).

DOI: 10.1039/b407246d

λ_{ex} and by scanning the monochromator that collects the luminescence emitted by the sample (black spectra in Fig. 1(c)). In the latter only a given emitted wavelength (λ_{emis}) is collected upon scanning the excitation λ_{ex} with a second monochromator located between the white source and the sample (grey spectra in Fig. 1(c)). Bulk ZnO exhibits a low efficient PL emission characterized by a broad band centred at 560 nm (17 860 cm^{-1}) which reaches its maximum intensity when excited in the ZnO gap 380 nm (26 300 cm^{-1}), dashed curves in Fig. 1(c).[12] Conversely, TADS exhibits a strong and complex PL emission composed of a dominant violet component at 400 nm (25 000 cm^{-1}) and a less intense, but still resolved, green emission at 500 nm (20 000 cm^{-1}) due to the aromatic rings (black dotted curve). The excitation scan (grey dotted curve) shows that the PL emission is at a maximum when λ_{ex} = 335 nm is used, which corresponds to the band gap of the material (Fig. 1(a)).

The MOF-5 material exhibits a significant PL in the broad 450–500 nm (22 220–16 660 cm^{-1}) interval, with a maximum at 525 nm (19 050 cm^{-1}, see the black solid curve in Fig. 1(c)). The 525 nm emission is more efficiently generated by exciting the sample with 350 nm (28 600 cm^{-1}) photons (grey solid curve). The intensity of the PL emission of MOF-5 is comparable to that of TADS and 16 times higher than that of ZnO. It is slightly blue shifted with respect to that of ZnO, while the dominant PL feature of the TADS is almost absent. Note that this emission occurs when the sample is illuminated with photons that are trapped by the organic part (the excitation spectra of MOF-5 and of TADS occur in the same spectral region). These features reveal an efficient energy transfer from the organic part of the framework, acting as a photon trap, to the inorganic Zn_4O_{13} QD, where the electron-hole recombination occurs, suggesting interesting optical applications of MOF-5.

Fig. 2 reports the Raman spectra of MOF-5, terephthalic acid, and TADS, obtained with different exciting lasers with wavelengths of 514 nm (19 450 cm^{-1}, solid spectra), 442 nm (22 625 cm^{-1}, dotted spectrum) and 325 nm (30 769 cm^{-1}, dashed spectrum). In the Raman spectra of terephthalic acid (curve 1), we can observe the modes associated with the carboxylate groups; in particular, the band at 1650 cm^{-1} is due to the C=O stretching, while the component at 1285 cm^{-1} is due to the stretching of C–O bonds. More complex are the vibrational finger prints of the benzene ring, which consist of the in-plane (1614, 1445, 1176 and 1120 cm^{-1}) and out-of-plane (827, 798 and 627 cm^{-1}) deformation modes of the C–H groups. When moving to the Raman spectrum of TADS (curve 2), the main differences observed can be summarized as follows: (i) a new doublet at 1598 and 1425 cm^{-1}, associated with the in- and out-of-phase stretching modes of the carboxylate group; (ii) a new band at 1133 cm^{-1}, probably due to a deformation mode involving the carboxylate group coupled with a C–C stretching mode; (iii) at lower Raman shifts, the out-of-plane deformation modes of the C–H groups appear at 863, 838, 820, 690, 640 and 630 cm^{-1}.

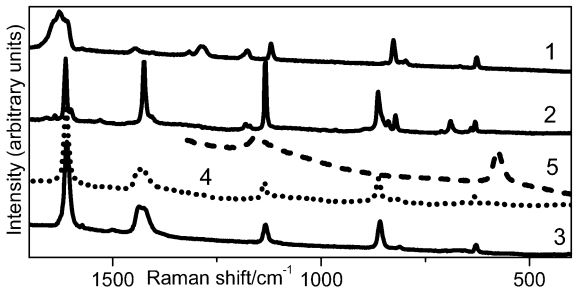

Fig. 2 Raman spectra of terephthalic acid (1), TADS (2) and MOF-5 (3–5). Solid, dotted and dashed lines refer to spectra collected with 514, 442 and 325 nm exciting lasers, respectively. The different spectra have been vertically shifted for graphical purposes.

The Raman spectrum of MOF-5, collected using the same green source (curve 3), is dominated by the vibration modes of the organic part, which undergo a simplification in the C–H stretching region, where only three components are observed at 860, 810 and 630 cm^{-1}. Analogous features are obtained using the blue line (curve 4). A dramatic change in the Raman spectra is observed by using a laser light able to excite the PL emission (Fig. 1(c)). Under such conditions all the previously described modes are totally overshadowed by the PL background and only two bands at 1155 and 578 cm^{-1} are strong enough to emerge. They must thus be subjected to resonant Raman effects which can increase the Raman efficiency by some orders of magnitude.[13] As 325 nm occurs in the LMCT of the ZnO-like QD (Fig. 1), and as the Raman spectra of both terephthalic acid and TADS only show the PL background, the 1155 and 578 cm^{-1} bands are inherently linked to modes associated with the Zn_4O_{13} group with a totally symmetric character.[13] A preliminary *ab initio* study indicates that the 1155 cm^{-1} component is a complex mode also involving the carboxylate stretching. For ZnO nanoparticles (4 nm), a Raman-enhanced band at 584 cm^{-1} has been observed exciting at λ = 364 nm.[14]

Acknowledgements are due to S. Bertarione, J. Vitillo and B. Civalleri for discussions and to R. Tagliapietra (Renishaw) for the 514 nm Raman spectra.

Notes and references

1 O. M. Yaghi, C. E. Davis, G. M. Li and H. L. Li, *J. Am. Chem. Soc.*, 1997, **119**, 2861; O. M. Yaghi, R. Jernigan, H. L. Li, C. E. Davis and T. L. Groy, *J. Chem. Soc., Dalton Trans.*, 1997, 2383.

2 M. J. Zaworotko, *Angew. Chem., Int. Ed.*, 2000, **39**, 3052.

3 O. M. Yaghi, M. O'Keeffe, N. W. Ockwig, H. K. Chae, M. Eddaoudi and J. Kim, *Nature*, 2003, **423**, 705.

4 G. Ferey, *Chem. Mater.*, 2001, **13**, 3084.

5 M. Eddaoudi, D. B. Moler, H. Li, B. Chen, T. M. Reineke, M. O'Keeffe and O. M. Yaghi, *Acc. Chem. Res.*, 2001, **34**, 319.

6 M. Eddaoudi, H. L. Li and O. M. Yaghi, *J. Am. Chem. Soc.*, 2000, **122**, 1391; J. Kim, B. L. Chen, T. M. Reineke, H. L. Li, M. Eddaoudi, D. B. Moler, M. O'Keeffe and O. M. Yaghi, *J. Am. Chem. Soc.*, 2001, **123**, 8239.

7 M. E. Braun, C. D. Steffek, J. Kim, P. G. Rasmussen and O. M. Yaghi, *Chem. Commun.*, 2001, 2532; D. T. Vodak, M. E. Braun, J. Kim, M. Eddaoudi and O. M. Yaghi, *Chem. Commun.*, 2001, 2534.

8 H. Li, M. Eddaoudi, M. O'Keeffe and O. M. Yaghi, *Nature*, 1999, **402**, 276.

9 J. S. Seo, D. Whang, H. Lee, S. I. Jun, J. Oh, Y. J. Jeon and K. Kim, *Nature*, 2000, **404**, 982; B. L. Chen, M. Eddaoudi, S. T. Hyde, M. O'Keeffe and O. M. Yaghi, *Science*, 2001, **291**, 1021; M. Eddaoudi, J. Kim, N. Rosi, D. Vodak, J. Wachter, M. O'Keeffe and O. M. Yaghi, *Science*, 2002, **295**, 469; N. L. Rosi, J. Eckert, M. Eddaoudi, D. T. Vodak, J. Kim, M. O'Keeffe and O. M. Yaghi, *Science*, 2003, **300**, 1127; H. K. Chae, D. Y. Siberio-Perez, J. Kim, Y. Go, M. Eddaoudi, A. J. Matzger, M. O'Keeffe and O. M. Yaghi, *Nature*, 2004, **427**, 523.

10 L. Huang, H. Wang, J. Chen, Z. Wang, J. Sun, D. Zhao and Y. Yan, *Microporous Mesoporous Mater.*, 2003, **58**, 105.

11 E. Borello, C. Lamberti, S. Bordiga, A. Zecchina and C. Otero Arean, *Appl. Phys. Lett.*, 1997, **71**, 2319; C. Lamberti, *Microporous Mesoporous Mater.*, 1999, **30**, 155; S. Bordiga, G. T. Palomino, A. Zecchina, G. Ranghino, E. Giamello and C. Lamberti, *J. Chem. Phys.*, 2000, **112**, 3859; A. Damin, F. X. L. Xamena, C. Lamberti, B. Civalleri, C. M. Zicovich-Wilson and A. Zecchina, *J. Phys. Chem. B*, 2004, **108**, 1328. As for ETS-10, the more consistent energy shift is due to the fact that the titanium oxide quantum wire is embedded in an insulating SiO_2 matrix: a less efficient confinement occurs for the electrons of the Zn_4O_{13} clusters in MOF-5.

12 D. W. Bahnemann, C. Kormann and M. R. Hoffmann, *J. Phys. Chem.*, 1987, **91**, 3789.

13 G. Ricchiardi, A. Damin, S. Bordiga, C. Lamberti, G. Spanò, F. Rivetti and A. Zecchina, *J. Am. Chem. Soc.*, 2001, **123**, 11409; S. Bordiga, A. Damin, F. Bonino, G. Ricchiardi, C. Lamberti and A. Zecchina, *Angew. Chem., Int. Ed.*, 2002, **41**, 4734.

14 M. Rajalakshmi, A. K. Arora, B. S. Bendre and S. Mahamuni, *J. Appl. Phys.*, 2000, **87**, 2445.